Journal of Superconductivity and Novel Magnetism (2022) 35:2679–2687
https://doi.org/10.1007/s10948-022-06317-2

ORIGINAL PAPER

Magnetic Ion Substitution and Peak Effect in YBCO: the Strange Case of $Y_{1-x}Gd_xBa_2Cu_3O_{7-\delta}$

D. M. Gokhfeld[1,2] · S. V. Semenov[1,2] · I. V. Nemtsev[1,2,3] · I. S. Yakimov[2] · D. A. Balaev[1,2]

Received: 12 April 2022 / Accepted: 29 May 2022 / Published online: 23 June 2022

Abstract
We present the results of a study of the superconducting and paramagnetic properties of polycrystalline $Y_{1-x}Gd_xBa_2Cu_3O_{7-\delta}$ samples. The critical current density and critical temperature of YBCO were weakly decreased by the Gd doping. A peak effect, which is a nonmonotonic dependence of the critical current density on magnetic field, was detected for all samples. The peak position shifted to higher magnetic fields with increasing Gd content. This behavior is opposite to the shift of the peak effect observed for other YBCO compounds doped by magnetic ions. This unusual behavior is apparently related to the realized granular structure instead of the type of doping ion. A correlation between the peak position and the granule size was found in the investigated samples and other polycrystalline YBCO compounds.

Keywords Peak effect · Bulk superconductors · Critical current · Pinning · X-ray diffraction · YBCO · Doping · Paramagnetic magnetization

1 Introduction

High values of the critical current density j_c in a superconductor require special defects, which are pinning centers for magnetic flux [1]. The main methods for creating structural defects are the introduction of nanoparticles into the material [2–8], the substitution of various cations into the crystal lattice [9–11], and the radiation exposure [12–14]. Pinning and the critical current density are affected by the size, arrangement, and magnetic order of the artificial defects [15–17]. For the $YBa_2Cu_3O_{7-\delta}$ (YBCO) superconductor, the substitution of homovalent rare earth ions (RE) for yttrium is used to improve pinning [18–20]. In contrast to this, some works reported that such substitution could suppress j_c [21, 22]. It may be agreed that the effect of the RE substitution on the critical current behavior is quite complex [23–25].

Let us list the results of work [21], wherein the detailed study of superconducting and magnetic properties of $Y_{1-x}Gd_xBa_2Cu_3O_{7-\delta}$ compounds was performed (these results are found to be almost valid for much YBCO compounds with other magnetic rare earth ions substituting Y).

(i) The samples behave as if they would consist of two non-interacting systems, one of them being superconducting and one of them being paramagnetic (such behavior is typical for superconductors with magnetic ions [26–28]).

(ii) The paramagnetic part of the $Y_{1-x}Gd_xBa_2Cu_3O_{7-\delta}$ samples is excellently described by the conventional theory of paramagnetism using the Brillouin function and assuming that the paramagnetic contribution to the magnetization exclusively arises from rare earth ions (see, e.g., [25, 29–31]).

(iii) The temperature dependence of the susceptibility above T_c follows a Curie–Weiss law with negative Curie–Weiss temperatures Θ (see, e.g., [25, 27]).

(iv) The critical current density decreases with increasing Gd content (as it was mentioned above the effect of doping is complex).

✉ D. M. Gokhfeld
gokhfeld@iph.krasn.ru

[1] Kirensky Institute of Physics, Federal Research Center KSC SB RAS, Krasnoyarsk 660036, Russia

[2] Siberian Federal University, Krasnoyarsk 660041, Russia

[3] Federal Research Center "Krasnoyarsk Science Center of the Siberian Branch of the Russian Academy of Sciences", Krasnoyarsk 660036, Russia

(v) The maximum in the $j_c(H)$ curve (the peak effect), occurring at a higher temperature, is shifted to lower magnetic fields with increasing Gd content (the similar shift of maximum in the $j_c(H)$ curve was observed for Nd and Ho-doped YBCO compounds [23, 25]. However, the position of maximum in the $j_c(H)$ curve of $Y_{1-x}Eu_xBa_2Cu_3O_{7-\delta}$ has nonmonotonic dependence on x [32]).

The investigated polycrystalline samples could have diversity in lattice parameters, sizes of granules, second phases, etc. A correct estimation of j_c of different samples and their comparison are required a diversity account for these parameters. It was supported early that a decrease of granule sizes may lead to an underestimation of j_c values [25, 33]. The peak effect may also depend on these parameters [34]. Some increase of the peak field with decreasing granule size was observed in $SmBa_2Cu_3O_{7-\delta}$ [34]. However, this effect was not studied in detail for $Y_{1-x}RE_xBa_2Cu_3O_{7-\delta}$.

Small concentrations of a doping element are expected to be most relevant to affect superconducting properties [35]. Nevertheless, these concentrations were poorly covered in works [21, 32]. A physically reliable non-uniform scale of the doping concentrations for YBCO was suggested in works [11, 36, 37]. These Petrov concentrations are linked with the average distance l_{ab} between the doping atoms in ab planes of crystallites as $x = a^2/{l_{ab}}^2 = N^2$, where a is the lattice constant and N is an integer number. In the presented study, we report structural, magnetic, and superconducting properties of $Y_{1-x}Gd_xBa_2Cu_3O_{7-\delta}$ using the Petrov concentrations. Correlations between different parameters have been observed, analyzed, and compared with the results obtained for other polycrystalline superconductors.

2 Experimental Methods

The solid-state synthesis was used to prepare $Y_{1-x}Gd_xBa_2Cu_3O_{7-\delta}$ samples from Y_2O_3, Gd_2O_3, $BaCO_3$, and CuO powders. Three stages of grinding, mixing, and heat treating during 10 h at 910 °C were performed to synthesize the samples with the Gd content $x = 0.02$, 0.11, and 0.25. The values of x are the same as the special concentrations used in the previous studies [23, 25, 38]. The values of $x = 0.02$, 0.11, and 0.25 correspond to $l_{ab} = 7a$, $3a$, and $2a$.

X-ray powder diffraction (XRD) data were obtained using XRD-7000S Shimadzu diffractometer (CuKα radiation). The 2θ angle ranged from 5 to 70° with a step of 0.02°. Scanning electron microscopy (SEM) investigations of the synthesized samples were carried out using a Hitachi TM4000Plus microscope. EDS spectrometer (Bruker) was used for energy dispersive spectrometry (EDS). EDS mapping data were obtained at 20 kV in 2 min. Fresh surfaces of the broken sample fragments were used for SEM and EDS.

Isothermal magnetization loops were obtained using a Quantum Design PPMS-9 T vibrating sample magnetometer. Temperature dependencies of the magnetization were measured with a Lakeshore VSM 8604 vibrating sample magnetometer.

3 Results and Discussion

3.1 X-ray Diffraction

Figure 1 shows X-ray diffraction patterns of the synthesized samples. All the patterns have identical positions of peaks. All the peaks correspond to the peaks in a reference pattern of the orthorhombic $YBa_2Cu_3O_{7-\delta}$ material (PDF2 ICDD #39–0486, space group Pmmm (47)—orthorhombic, cell parameters: $a = 3.8877$ Å, $b = 3.8214$ Å, $c = 11.693$ Å). The

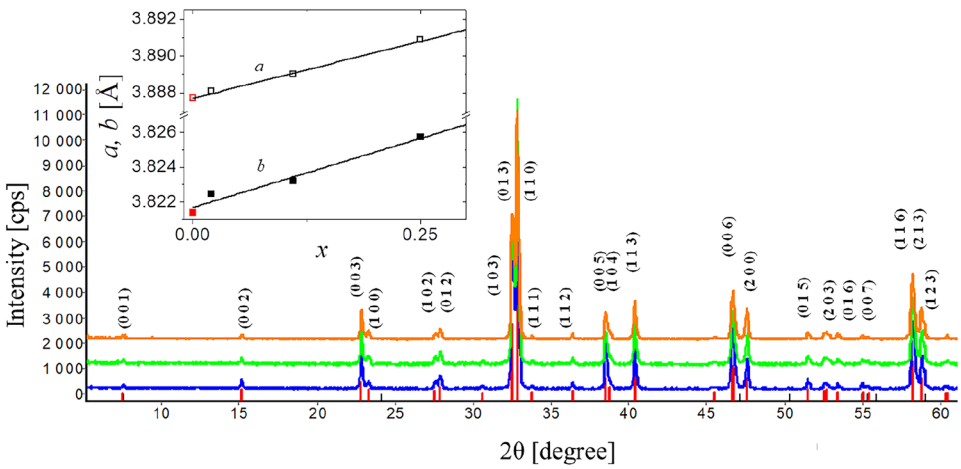

Fig. 1 X-ray diffraction. From bottom to top: $x = 0.02$, 0.11, 0.25. For clarity, curves are shifted along the intensity axis. Red marks indicate the $YBa_2Cu_3O_{6.96}$ reference. The lattice parameters a and b versus x are shown on the inset

compositions of the samples and cell parameters were specified using the Rietveld method. The results of XRD analysis are presented in Table 1. Distortions of the crystal lattice due to the substitution of Gd for Y in $Y_{1-x}Gd_xBa_2Cu_3O_{7-\delta}$ are quite weak. The lattice parameter a grows only on 0.072% as x increases from 0.02 to 0.25. The inset of Fig. 1 shows that the dependence of the parameter a on x is linear as well as the dependence of b on x. Such linear dependence of the lattice parameters on x indicates that Gd is completely dissolved in the $Y_{1-x}Gd_xBa_2Cu_3O_{7-\delta}$ compound. As verified by XRD, the real compositions comply with the nominal.

The lattice parameter c of the Y-123 lattice depends mostly on the oxygen content 7–δ and this dependence is described by the empirical relation 7–δ = 75.250 – 5.856c [39]. We have estimated the oxygen content using this equation and the results are given in Table 1.

3.2 SEM and EDS

SEM images of the samples are shown in Fig. 2a–c. The samples have a disordered granular structure. For all the samples, the granule sizes are distributed from 1 to 20 μm; the average granule size is about 3 μm.

The EDS images confirm the uniform distribution of Gd over granules for all samples. Figure 2d shows a typical EDS image of the sample with $x = 0.25$.

3.3 Temperature Dependence of Magnetization

The inset of Fig. 3a shows temperature dependencies of the magnetization $M(T)$ measured under zero field cooled conditions in a magnetic field of 0.001 T. The superconducting transition temperature T_c determined from temperature dependencies of magnetization is about 93 K for all the samples (see Table 1). The same magnetization level at the lowest temperature means similar porosity of all the samples.

The $M(T)$ dependencies measured under zero field cooled conditions in a magnetic field of 1 T in temperature range 100–300 K are demonstrated in Fig. 3b. The magnetization above T_c is apparently due to the magnetic moment paramagnetic ions [21, 23, 40]. The paramagnetic $M(T)$ dependencies above T_c were described by the function:

$$M_P(H,T) = Ng_L J\mu_B B_J\left(\frac{g_L J\mu_B\mu_0 H}{k_B(T-\Theta)}\right), \quad (1)$$

where N is a number of magnetic ions per unit volume, μ_B is the Bohr magneton, k_B is the Boltzmann constant, g_L is a Lande g-factor, J is an angular momentum quantum number, B_J is the Brillouin function, and Θ is a Curie–Weiss temperature used to be the fitting parameter. Solid curves on Fig. 5 are given by relation (1) with parameters for Gd^{3+} ions ($J = 3.5$ and $g_L = 2$) and $N = 5.76 \cdot 10^{27} \cdot x\ m^{-3}$. Fitting values of

Table 1 Characterization of samples

x	Cell parameter a, Å	Cell parameter b, Å	Cell parameter c, Å	Cell volume, Å^3	Oxygen content 7–δ	Critical temperature T_c, K	Curie–Weiss temperature Θ, K	Critical current density j_c at 4.2 K, 10^6 A cm^{-2}	Average size of granules d, μm	Transition field H_{peak} at 60 K, T
0.02	3.88807	3.82248	11.69454	173.805	6.767	93.8 ± 0.4	–29	18.3	4.1	4.89
0.11	3.88901	3.82321	11.69450	173.880	6.767	93.1 ± 0.3	–8	15.6	3.0	5.83
0.25	3.89087	3.82572	11.69813	174.131	6.746	93.1 ± 0.3	–8	18.1	2.7	8.05

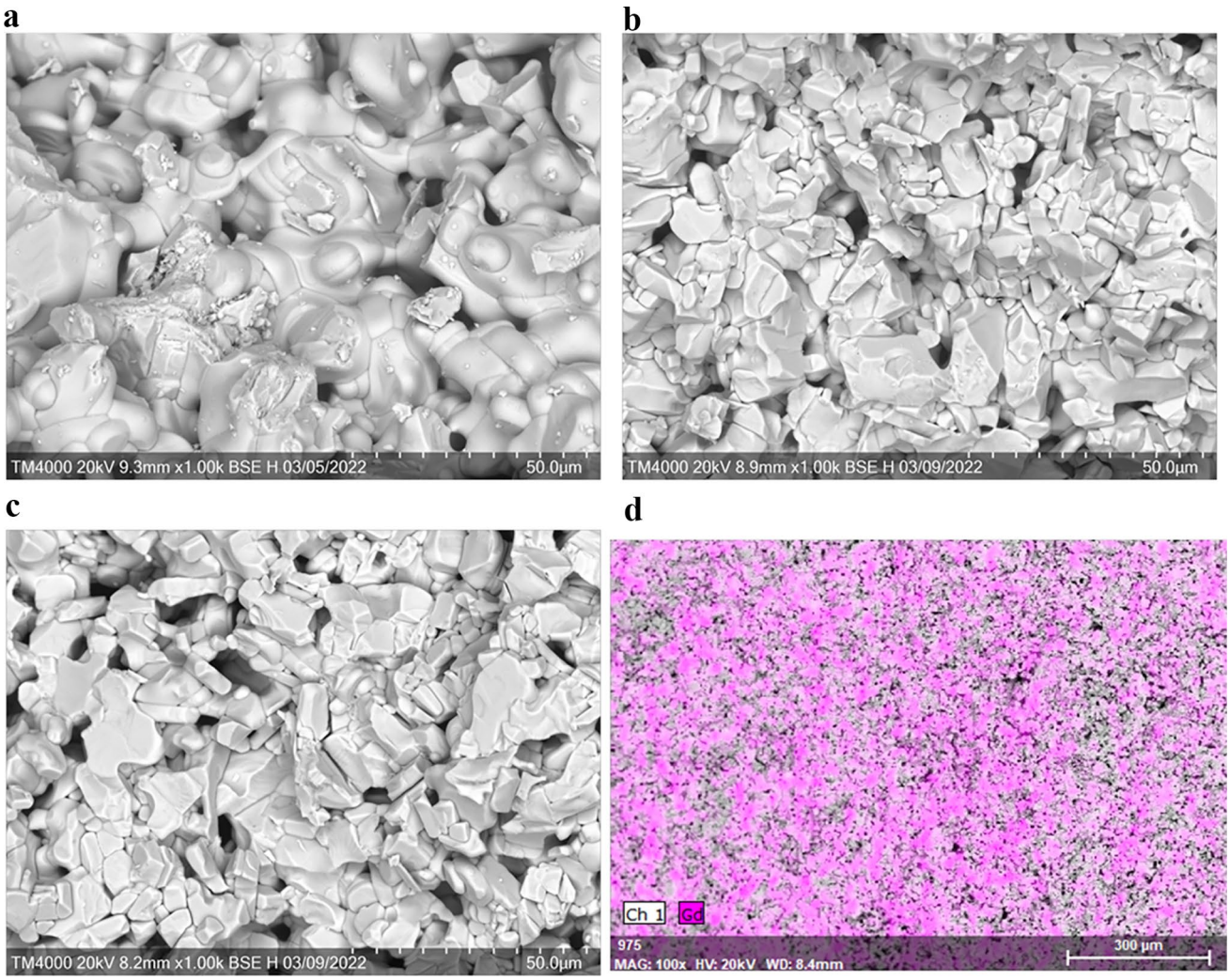

Fig. 2 SEM images of **a** $x=0.02$, **b** $x=0.11$, and **c** $x=0.25$ and **d** EDS image of $x=0.25$. The pink color marks the Gd distribution in the sample

Θ are given in Table 1. As can be seen, the experimental data for $x=0.02$ and $x=0.25$ are successfully fitted by (1). Agreement between the experimental dependence and computed curve for $x=0.11$ is some worse. Also a temperature dependence of the inverse susceptibility $\chi^{-1}=(M/H)^{-1}$ is linear for $x=0.02$ and $x=0.25$, but diverges from a line for $x=0.11$.

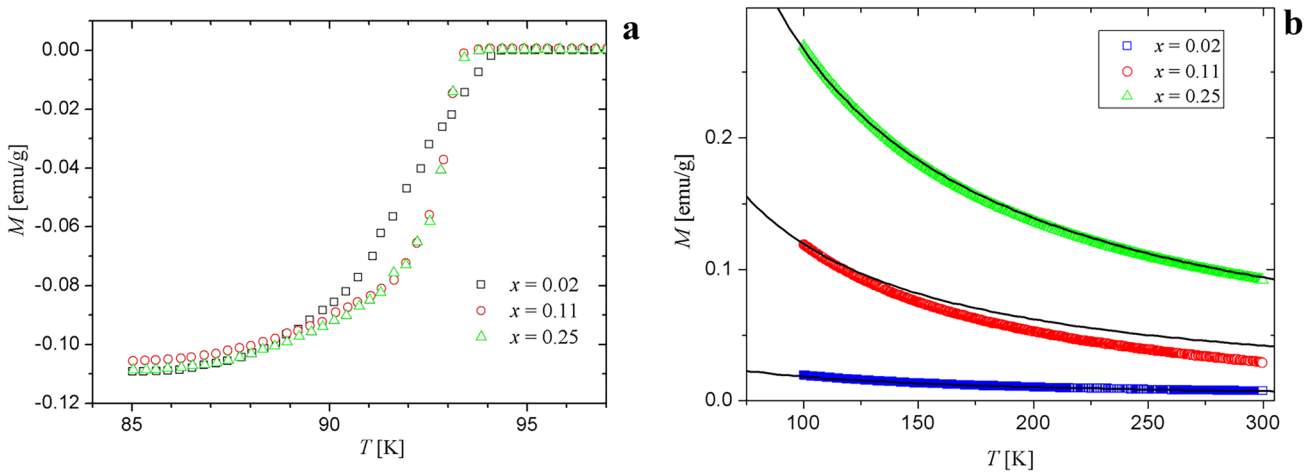

Fig. 3 Temperature dependencies of magnetization: **a** $T<100$ K, $\mu_0 H=1$ mT, **b** $T>100$ K, $\mu_0 H=1$ T

We believe that the negative value of Θ for $x = 0.25$ indicates antiferromagnetic correlations between rare earth ions in YBCO [21, 25]. The samples with $x = 0.02$ and $x = 0.11$ may have other sources of negative Θ (Pauli paramagnetism, Van Vleck paramagnetism, etc.) [41].

3.4 Magnetization Hysteresis Loops

Figure 4a–e show magnetic hysteresis loops (MHLs) for the $Y_{1-x}Gd_xBa_2Cu_3O_{7-\delta}$ samples in the temperature range of 20 – 80 K. The isothermal magnetization loops are tilted anticlockwise and their tilt increases with x. We may conclude that one magnetic subsystem formed by the paramagnetic Gd ions and the other formed by the superconducting granules contribute to MHLs.

The superconducting magnetization was determined from the experimental MHLs as $M_S(H) = M(H) - M_P(H)$, where $M_P(H)$ is given by (1). Providing only $\Theta = 0$, there is no tilt of resulted superconducting MHLs in high fields H. The resulted MHLs of the superconducting subsystem are plotted on Fig. 5.

The $\Theta = 0$ condition means that antiferromagnetic correlations are probably blocked below T_c. A possible modification of the electronic spectrum [42] may be a reason of this blocking. The superconducting screening, which decreases the paramagnetic magnetization [25, 30], is quite low for these compounds (no less than 90% of Gd ions contribute to the magnetization).

3.5 Critical Current Density and Pinning Force Density

The critical current density j_c was determined from the experimental MHLs using the Bean formula:

$$j_c = 3\Delta M/d, \tag{2}$$

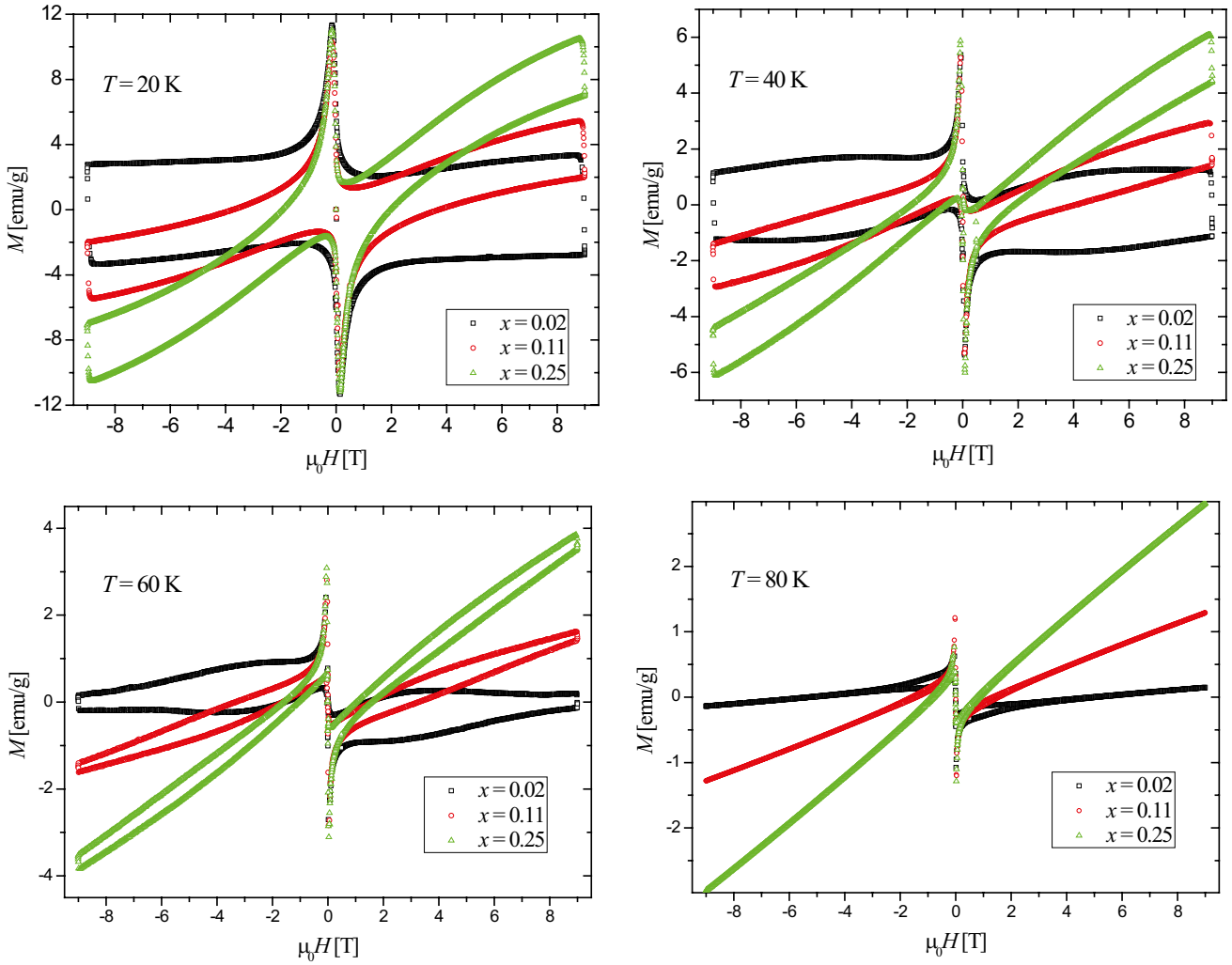

Fig. 4 Magnetization hysteresis loops at four different temperatures

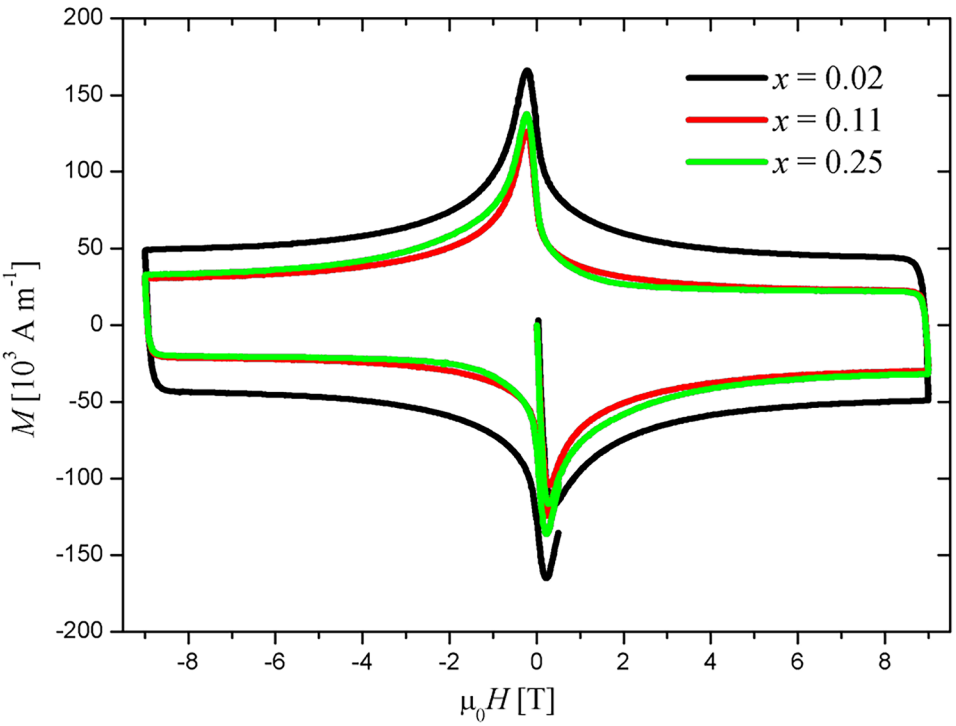

Fig. 5 Magnetic hysteresis loops of superconducting subsystem at $T = 4.2$ K

where ΔM is the difference between the ascending and descending hysteresis branches and d is the characteristic size of current circulation. Variation of the physical density of $Y_{1-x}Gd_xBa_2Cu_3O_{7-\delta}$ (6.36 g/cm^3 for $x = 0.02$, 6.42 g/cm^3 for $x = 0.11$, and 6.51 g/cm^3 for $x = 0.25$) was accounted to convert experimental values of the magnetic moment and the mass to the volume magnetization M. The d values were calculated by means of the method [33]:

$$d \approx 2\lambda_L/[1 - |0.5\Delta M/Mmin|^{1/3}], \quad (3)$$

where λ_L is the London penetration depth, and M_{min} is the low-field peak magnetization. The values of d presented in Table 1 are about the average granule size observed on the SEM figures. The resulting $j_c(H)$ dependencies are presented on Fig. 6a. The maximal values of j_c are also given in Table 1.

If one uses a constant value of d in Eq. (2), as it was done in some works (e.g., [21]), then the estimated values of j_c at $T = 4.2$ K would decrease on 35% as x increases from 0.02 to 0.25. However, such a strong effect is not correct. Taking

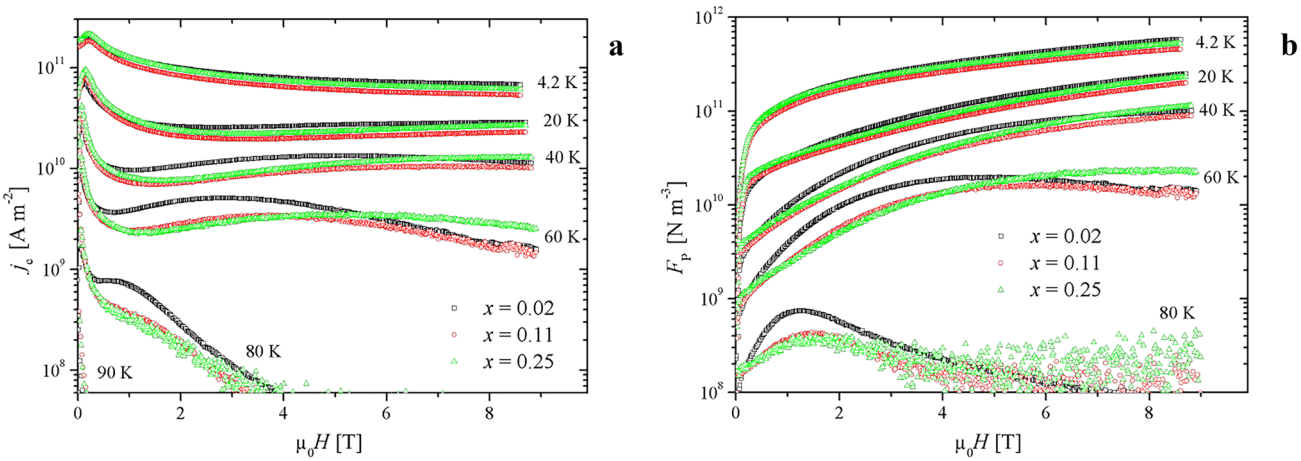

Fig. 6 Magnetic field dependencies of **a** critical current density and **b** pinning force density

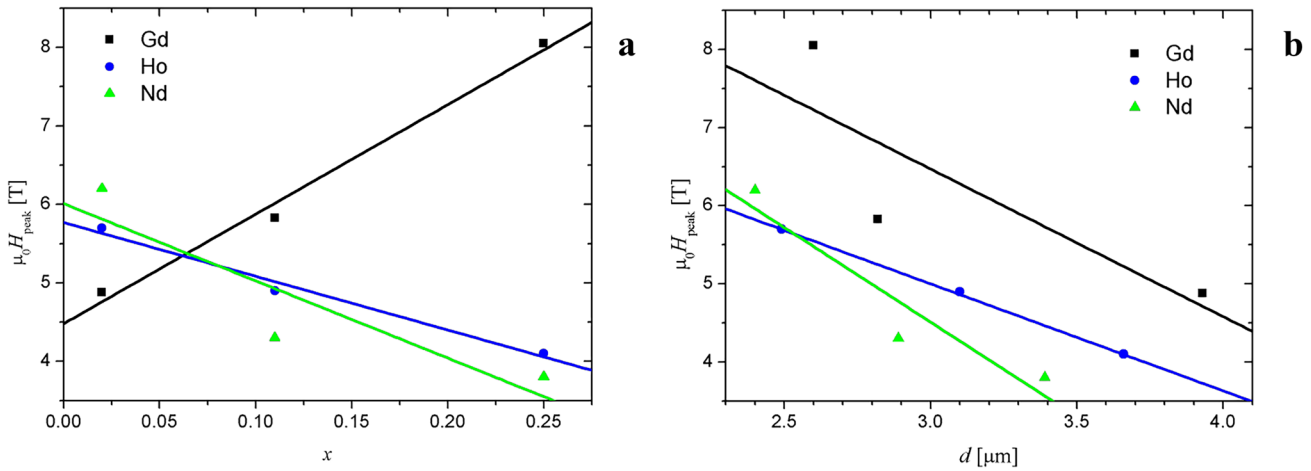

Fig. 7 The peak field versus the RE content **a** and versus the grain size **b** in different $Y_{1-x}RE_xBa_2Cu_3O_{7-\delta}$. Lines are linear approximations

into account the diversity of d, the estimated values of j_c decrease by only 1.1%.

The $j_c(H)$ dependencies at some temperatures demonstrated non-monotonic behavior, the peak effect. They had a maximum corresponding to the fishtail feature on MHSs at high fields [43, 44]. For YBCO compounds, the peak effect is usually attributed to transitions of the Abrikosov vortex lattice [23, 45–47]. The transition field may be related to a maximum of the pinning force at $H = H_{peak}$. The pinning force density F_p is determined by $F_p(H) = \mu_0 H j_c(H)$. The $F_p(H)$ dependencies are plotted on Fig. 6b. As can be seen, the maximum was reached only for the $F_p(H)$ curves at $T = 60$ K (see Table 1) and 80 K, i.e., $\mu_0 H_{peak} \leq 9$ T for these curves.

3.6 Shift of the Peak Effect with Increasing RE Content

The transition field H_{peak} was found to depend on the Gd content x. H_{peak} monotonically increased with increasing x (square points in Fig. 7a demonstrate the values of H_{peak} at 60 K; a similar behavior of H_{peak} is found at 80 K). This behavior does not agree with the previous results for the related compounds $Y_{1-x}Nd_xBa_2Cu_3O_{7-\delta}$ and $Y_{1-x}Ho_xBa_2Cu_3O_{7-\delta}$ (triangle and circle points in Fig. 7a demonstrate the values of H_{peak} at 60 K for these compounds). This contradiction means that a correlation between H_{peak} and x is more complicated than it was believed in previous works. Earlier, we suggested that magnetic ions modify an effective magnetic field in the doped superconductors. However, recent work called this idea into question; it is supported [48] that the doping paramagnetic ions do not affect the superconducting environment. So we assume that another parameter controls the H_{peak} value in the investigated samples.

Competition between bulk and surface pinning may affect the position of the peak effect [49, 50]. The contribution of surface pinning in polycrystalline superconductors depends on the average granule size. Furthermore, the granule size makes it possible to govern characteristic fields of the order–disorder transition [23, 25, 31, 34]. The contribution of surface pinning is higher for smaller granules. This contribution reduces the field of the order–disorder transition of vortex lattice.

We plot the dependence of x on the estimated granule size d for available experimental data comprising $Y_{1-x}Gd_xBa_2Cu_3O_{7-\delta}$, $Y_{1-x}Nd_xBa_2Cu_3O_{7-\delta}$ [23], and $Y_{1-x}Ho_xBa_2Cu_3O_{7-\delta}$ [25] (Fig. 7b). Apparent correlation between the transition field and the granule size is observed for all the samples. The samples with smaller granules have higher values of H_{peak}. This behavior agrees with the increasing contribution of surface pinning [49, 50].

The connection between H_{peak} and x may be determined by synthesis conditions. Peak-effect depends on a structural disorder in superconductors [45]. Furthermore, the melting temperature of RE-substituted YBCO depends on the sort and the content of the substituting RE [29, 30]. This leads to different growth rates during synthesis, different average granule sizes, and correspondingly different values of H_{peak} in polycrystalline $Y_{1-x}RE_xBa_2Cu_3O_{7-\delta}$.

4 Conclusions

Polycrystalline $Y_{1-x}Gd_xBa_2Cu_3O_{7-\delta}$ ($x = 0.02$, 0.11, and 0.25) superconductors were synthesized and characterized. The results of XRD, EDX, and M–T measurements indicate that the Gd ions are successfully replaced by the yttrium sites in the crystal lattice of YBCO.

Two magnetic subsystems were detected in these compounds: the paramagnetic subsystem formed by Gd atoms and the superconducting subsystem residing at a whole sample. The paramagnetic part of the $Y_{1-x}Gd_xBa_2Cu_3O_{7-\delta}$ samples was described by the conventional theory of paramagnetism of Gd^{3+} ions. The temperature dependence of the susceptibility above T_c followed the Curie–Weiss law with negative Curie–Weiss temperatures Θ. The magnetization width ΔM of hysteresis loops and the position of maximum H_{peak} were changed with increasing magnetic ion content. In contrast to the previous studies [21, 23, 25, 28], the granule size is established to be the primary factor affecting ΔM and H_{peak}. The granule size is sensitive to the Gd content because admixtures change the melting temperature and the growth rate during synthesis.

Acknowledgements We are thankful to Yu.S. Gokhfeld, K.Yu. Terentyev, and M.I. Petrov for assistance in the sample preparation. SEM and magnetic measurements were carried out at the Krasnoyarsk Regional Center of Research Equipment, Federal Research Center "Krasnoyarsk Science Center SB RAS."

Funding This work was supported by the Russian Foundation for Basic Research and the Government of the Krasnoyarsk Territory, Krasnoyarsk Territorial Foundation for Support of Scientific and R&D Activities, project "Superconducting properties of YBCO incorporated by paramagnetic rare-earth elements" No. 20–42-240008.

Data Availability The data that support the findings of this study are available from the corresponding author upon reasonable request.

Declarations

Conflict of Interest The authors declare no competing interests.

References

1. Kwok, W.K., Welp, U., Glatz, A., Koshelev, A.E., Kihlstrom, K.J., Crabtree, G.W.: Vortices in high-performance high-temperature superconductors. Reports Prog. Phys. **79**, 116501 (2016). https://doi.org/10.1088/0034-4885/79/11/116501
2. Haugan, T., Barnes, P.N., Wheeler, R., Meisenkothen, F., Sumption, M.: Addition of nanoparticle dispersions to enhance flux pinning of the YBa2Cu3O7-x superconductor. Nature **430**, 867–870 (2004). https://doi.org/10.1038/nature02792
3. Koshelev, A.E., Kolton, A.B.: Theory and simulations on strong pinning of vortex lines by nanoparticles. Phys. Rev. B. **84**, 104528 (2011). https://doi.org/10.1103/PhysRevB.84.104528
4. Surdu, A.E., Hamdeh, H.H., Al-Omari, I.A., Sellmyer, D.J., Socrovisciuc, A.V., Prepelita, A.A., Koparan, E.T., Yanmaz, E., Ryazanov, V.V., Hahn, H., Sidorenko, A.S.: Enhancement of the critical current density in FeO-coated MgB2 thin films at high magnetic fields. Beilstein J. Nanotechnol. **289**(2), 809–813 (2011). https://doi.org/10.3762/BJNANO.2.89
5. Taylan Koparan, E., Surdu, A., Awawdeh, A., Sidorenko, A., Yanmaz, E.: Artificial pinning centers on MgB 2 superconducting thin films coated by FeO nanoparticles. J. Supercond. Nov. Magn. **25**, 1761–1767 (2012). https://doi.org/10.1007/S10948-012-1533-1/FIGURES/7
6. Taylan Koparan, E., Surdu, A., Sidorenko, A., Yanmaz, E.: Artificial pinning centers created by Fe2O3 coating on MgB2 thin films. Phys. C Supercond. **473**, 1–5 (2012). https://doi.org/10.1016/J.PHYSC.2011.11.004
7. Altin, E., Gokhfeld, D.M., Komogortsev, S.V., Altin, S., Yakinci, M.E.: Hysteresis loops of MgB2 + Co composite tapes. J. Mater. Sci. Mater. Electron. **24**, 1341–1347 (2013). https://doi.org/10.1007/s10854-012-0931-2
8. Lepeshev, A.A., Patrin, G.S., Yurkin, G.Y., Vasiliev, A.D., Nemtsev, I.V., Gokhfeld, D.M., Balaev, A.D., Demin, V.G., Bachurina, E.P., Karpov, I.V., Ushakov, A.V., Fedorov, L.Y., Irtyugo, L.A., Petrov, M.I.: Magnetic properties and critical current of superconducting nanocomposites (1–x)YBa2Cu3O7−δ + xCuO. J. Supercond. Nov. Magn. **31**, 3841–3845 (2018). https://doi.org/10.1007/s10948-018-4676-x
9. Sidorenko, A., Scheidt, E.W., Haider, F., Klemm, M., Horn, S., Konopko, L., Tidecks, R.: The effect of Cu/Mn substitution in 2223 Bi-based HTSC. Phys. B Condens. Matter. **321**, 298–300 (2002). https://doi.org/10.1016/S0921-4526(02)00865-7
10. Huhtinen, H., Awana, V.P.S., Gupta, A., Kishan, H., Laiho, R., Narlikar, A.V.: Pinning centres and enhancement of critical current density in YBCO doped with Pr. Caand Ni. Supercond. Sci. Technol. **20**, S159 (2007). https://doi.org/10.1088/0953-2048/20/9/S08
11. Petrov, M.I., Gokhfeld, Y.S., Balaev, D.A., Popkov, S.I., Dubrovskiy, A.A., Gokhfeld, D.M., Shaykhutdinov, K.A.: Pinning enhancement by heterovalent substitution in Y1-xRExBa2Cu3O7-δ. Supercond. Sci. Technol. **21**, (2008). https://doi.org/10.1088/0953-2048/21/8/085015
12. Moshensky, A.A., Tischenko, L.P., Sidorenko, A.S., Fogel, N.Y.: Critical currents of thin films and their connection with inhomogeneities of superconductor. Sov. J. Phys. Sol. State. **3**, 418–427 (1976)
13. Freyhardt, H.C.: Radiation-induced flux pinning in type II superconductors. J. Low Temp. Phys. **32**, 101–129 (1978). https://doi.org/10.1007/BF00116908
14. Fischer, D.X., Prokopec, R., Emhofer, J., Eisterer, M.: The effect of fast neutron irradiation on the superconducting properties of REBCO coated conductors with and without artificial pinning centers. Supercond. Sci. Technol. **31**, 044006 (2018). https://doi.org/10.1088/1361-6668/aaadf2
15. Uspenskaya, L., Naumenko, I., Emelchenko, G., Boguslavskii, Y., Zver'kov, S., Yakimov, E., Litzkendorf, D., Gawalek, W., Caplin, A.: Effect of mesoscopic inhomogeneities on the critical current of bulk melt-textured YBCO. Phys. C Supercond. **390**, 127–133 (2003). https://doi.org/10.1016/S0921-4534(03)00629-4
16. Hoffmann, A., Prieto, P., Metlushko, V., Schuller, I.K.: Superconducting vortex pinning with magnetic dots: does size and magnetic configuration matter? J. Supercond. Nov. Magn. **25**, 2187–2191 (2012). https://doi.org/10.1007/s10948-012-1647-5
17. Maksimova, A.N., Kashurnikov, V.A., Moroz, A.N., Gokhfeld, D.M.: Trapped field in superconductors with perforations. J. Supercond. Nov. Magn. **35**, 283–290 (2022). https://doi.org/10.1007/s10948-021-06067-7
18. Yong, F., Lian, Z.: Superconducting properties and microstructures of the powder melting processed YHoBaCuO and YGdBaCuO superconductors. Phys. C Supercond. **202**, 298–302 (1992). https://doi.org/10.1016/0921-4534(92)90174-B
19. Goodilin, E.A., Kvartalov, D.B., Oleynikov, N.N., Tretyakov, Y.D.: Modified melt techniques for high Jc YBCO preparation. Phys. C Supercond. **235–240**, 449–450 (1994). https://doi.org/10.1016/0921-4534(94)91448-6
20. Öztürk, K., Çelik, Ş, Çevik, U., Yanmaz, E.: The effect of Gd diffusion-doped on structural and superconducting properties of YBa2Cu3O7−x superconductors. J. Alloys Compd. **433**, 46–52 (2007). https://doi.org/10.1016/J.JALLCOM.2006.06.082

21. Theuss, H., Kronmüller, H.: Magnetic properties of Y1-xGdxBa2Cu3O7-δ polycrystals. Phys. C Supercond. its Appl. **242**, 155–163 (1995). https://doi.org/10.1016/0921-4534(94)02404-9
22. Öztürk, A., Doğan, M., Düzgün, İ, Çelebi, S.: The effect of Dy doping on the magnetic behavior of YBCO superconductors. J. Supercond. Nov. Magn. **29**, 1787–1791 (2016). https://doi.org/10.1007/s10948-016-3493-3
23. Gokhfeld, D.M., Balaev, D.A., Yakimov, I.S., Petrov, M.I., Semenov, S.V.: Tuning the peak effect in the Y1−xNdxBa2Cu3O7−δ compound. Ceram. Int. **43**, 9985–9991 (2017). https://doi.org/10.1016/J.CERAMINT.2017.05.011
24. Zhang, S., Xu, S., Fan, Z., Jiang, P., Han, Z., Yang, G., Chen, Y.: Broad temperature study of RE-substitution effects on the in-field critical current behavior of REBCO superconducting tapes. Supercond. Sci. Technol. **31**, 125006 (2018). https://doi.org/10.1088/1361-6668/AAE460
25. Gokhfeld, D.M., Semenov, S.V., Terentyev, K.Y., Yakimov, I.S., Balaev, D.A.: Interplay of magnetic and superconducting subsystems in Ho-doped YBCO. J. Supercond. Nov. Magn. **34**, 2537–2543 (2021). https://doi.org/10.1007/S10948-021-05954-3/FIGURES/7
26. Senoussi, S., Sastry, P.V.S.S., Yakhmi, J.V., Campbell, I.A.: Magnetic hysteresis of superconducting GdBa2Cu3O7 down to 1.8 K. Le J. Phys. Colloq. **49**, C8–2163-C8–2164 (1988). https://doi.org/10.1051/jphyscol:19888969
27. Singh, K., Hermes, W., Kaushik, S.D., Balamurugan, S., Bhattacharya, S., Gaur, N.K., Rayaprol, S., Pöttgen, R.: Superconductivity and magnetism in R 2CaBa2Cu5O z (R=La, Pr, Nd and Eu). J. Supercond. Nov. Magn. **22**(8), 759–767 (2009). https://doi.org/10.1007/S10948-009-0493-6
28. Gokhfeld, D.M., Semenov, S.V., Balaev, D.A., Yakimov, I.S., Dubrovskiy, A.A., Terentyev, K.Y., Freydman, A.L., Krasikov, A.A., Petrov, M.I.: Establishing of peak effect in YBCO by Nd substitution. J. Magn. Magn. Mater. **440**, 127–128 (2017). https://doi.org/10.1016/j.jmmm.2016.12.089
29. Altin, E., Gokhfeld, D.M., Demirel, S., Oz, E., Kurt, F., Altin, S., Yakinci, M.E.: Vortex pinning and magnetic peak effect in Eu(Eu,Ba)2.125Cu3Ox. J. Mater. Sci. Mater. Electron. **25**, 1466–1473 (2014). https://doi.org/10.1007/s10854-014-1753-1
30. Altin, E., Gokhfeld, D.M., Kurt, F., Yakinci, Z.D.: Physical, electrical, transport and magnetic properties of Nd(Ba,Nd)2.1Cu3O7−δ system. J. Mater. Sci. Mater. Electron. **24**, 5075–5084 (2013). https://doi.org/10.1007/s10854-013-1526-2
31. Hyun, O.B., Hirabayashi, I.: Effects of local moments on the magnetization of HoBa2Cu3O7. Phys. Rev. B. **50**, 16023–16027 (1994). https://doi.org/10.1103/PhysRevB.50.16023
32. Li, Y., Perkins, G.K., Caplin, A.D., Cao, G., Ma, Q., Wei, L., Zhao, Z.X.: Study of the pinning behaviour in yttrium-doped Eu-123 superconductors. Supercond. Sci. Technol. **13**, 1029–1034 (2000). https://doi.org/10.1088/0953-2048/13/7/321
33. Gokhfeld, D.M.: The circulation radius and critical current density in type II superconductors. Tech. Phys. Lett. **45**, 1–3 (2019). https://doi.org/10.1134/S1063785019010243
34. Matsushita, T., Otabe, E.S., Wada, H., Takahama, Y., Yamauchi, H.: Size dependencies of the peak effect and irreversibility field in superconducting Sm-123 powders. Phys. C Supercond. **397**, 38–46 (2003). https://doi.org/10.1016/S0921-4534(03)01085-2
35. Barnes, P.N., Kell, J.W., Harrison, B.C., Haugan, T.J., Varanasi, C.V., Rane, M., Ramos, F.: Minute doping with deleterious rare earths in YBa2Cu3O7−δ films for flux pinning enhancements. Appl. Phys. Lett. **89**, 012503 (2006). https://doi.org/10.1063/1.2219391
36. Petrov, M.I., Balaev, D.A., Gokhfel'd, Y.S., Dubrovskiĭ, A.A., Sha'khutdinov, K.A.: Effect of heterovalent substitution of rare-earth elements on the magnetic and transport properties of YBa2Cu3O7. Phys. Solid State. **49**, 2047–2051 (2007). https://doi.org/10.1134/S1063783407110054
37. Petrov, M.I., Balaev, D.A., Gokhfeld, Y.S., Dubrovskiy, A.A., Shaykhutdinov, K.A.: Enhancement of pinning in cerium doped Y(1–x)CexBa2Cu3O7 HTSC. Phys. C Supercond. **460–462**, 1192–1193 (2007). https://doi.org/10.1016/J.PHYSC.2007.04.046
38. Gokhfeld, D.: Use of a sigmoid function to describe second peak in magnetization loops. (2017)
39. Benzi, P., Bottizzo, E., Rizzi, N.: Oxygen determination from cell dimensions in YBCO superconductors. J. Cryst. Growth. **269**, 625–629 (2004). https://doi.org/10.1016/J.JCRYSGRO.2004.05.082
40. Sandu, V., Popa, S., Di Gioacchino, D., Tripodi, P.: Paramagnetism and superconductivity in Eu 0.7Sm 0.3Ba 2Cu 3O 7-δ. J. Supercond. Nov. Magn. **17**, 701–710 (2004). https://doi.org/10.1007/s10948-004-0830-8
41. Mamsurova, L.G., Trusevich, N.G., Pigalskiy, K.S., Vishnev, A.A., Gadzhimagomedov, S.K., Murlieva, Z.K., Palchaev, D.K., Bugaev, A.S.: Magnetization and static magnetic susceptibility of fine-crystalline high-temperature YBa2Cu3Oy superconductors synthesized by the sol–gel method. Russ. J. Phys. Chem. B. **12**, 908–915 (2018). https://doi.org/10.1134/S1990793118050081
42. Bourges, P., Sidis, Y., Fong, H.F., Regnault, L.P., Bossy, J., Ivanov, A., Keimer, B.: The spin excitation spectrum in superconducting YBa2Cu3O6.85. Science (80-.). **288**, 1234–1237 (2000). https://doi.org/10.1126/science.288.5469.1234
43. Gokhfeld, D.M.: Secondary peak on asymmetric magnetization loop of type-II superconductors. J. Supercond. Nov. Magn. **26**, 281–283 (2013). https://doi.org/10.1007/s10948-012-1741-8
44. Gokhfeld, D.: Use of a sigmoid function to describe second peak in magnetization loops. J. Supercond. Nov. Magn. **31**, 1785–1789 (2018). https://doi.org/10.1007/s10948-017-4400-2
45. Koshelev, A.E., Vinokur, V.M.: Pinning-induced transition to disordered vortex phase in layered superconductors. Phys. Rev. B. **57**, 8026–8033 (1998). https://doi.org/10.1103/PhysRevB.57.8026
46. Babich, I.M., Brandt, E.H., Mikitik, G.P., Zeldov, E.: Critical current in type-II superconductors near the order-disorder transition. Phys. Rev. B. **81**, 054517 (2010). https://doi.org/10.1103/PhysRevB.81.054517
47. Ionescu, A.M., Miu, D., Crisan, A., Miu, L.: Pinning-induced vortex-system disordering at the origin of the second magnetization peak in superconducting single crystals. J. Supercond. Nov. Magn. 1–9 (2017). https://doi.org/10.1007/s10948-017-4487-5
48. Semenov, S.V., Gokhfel'd, D.M., Terent'ev, K.Y., Balaev, D.A.: Mechanisms of the magnetoresistance hysteresis in a granular HTS with the paramagnetic contribution by the example of HoBa2Cu3O7 – δ. Phys. Solid State. **63**, 1785–1794 (2021). https://doi.org/10.1134/S1063783421100334/FIGURES/9
49. Aĭnbinder, R.M., Vodolazov, D.Y., Maksimov, I.L.: Low-field peak effect in type II superconductors. Tech. Phys. 2005 507. **50**, 954–956 (2013). https://doi.org/10.1134/1.1994981
50. Maksimov, I.L., Ainbinder, R.M., Vodolazov, D.Y.: Anomalous peak-effect in type-II superconductors: a competition between bulk pinning and a surface barrier. Phys. C Supercond. Appl. **451**, 127–133 (2007). https://doi.org/10.1016/J.PHYSC.2006.11.005